

12-2009

# Space Charge Polarization Measurements as a Method to Determine the Temperature Dependence of the Number Density of Mobile Cations in Ion Conducting Glasses

Steve W. Martin

*Iowa State University*, [swmartin@iastate.edu](mailto:swmartin@iastate.edu)

Wenlong Yao

*Iowa State University*

Kyle Berg

*Iowa State University*

Follow this and additional works at: [http://lib.dr.iastate.edu/mse\\_pubs](http://lib.dr.iastate.edu/mse_pubs)



Part of the [Materials Science and Engineering Commons](#)

The complete bibliographic information for this item can be found at [http://lib.dr.iastate.edu/mse\\_pubs/157](http://lib.dr.iastate.edu/mse_pubs/157). For information on how to cite this item, please visit <http://lib.dr.iastate.edu/howtocite.html>.

---

This Article is brought to you for free and open access by the Materials Science and Engineering at Iowa State University Digital Repository. It has been accepted for inclusion in Materials Science and Engineering Publications by an authorized administrator of Iowa State University Digital Repository. For more information, please contact [digirep@iastate.edu](mailto:digirep@iastate.edu).

---

# Space Charge Polarization Measurements as a Method to Determine the Temperature Dependence of the Number Density of Mobile Cations in Ion Conducting Glasses

## Abstract

A method is proposed using mean-field theories to help solve a long standing problem in the study of ionically solid electrolytes. While it has been long known that the ionic conductivity in solid electrolytes is comprised of two terms, the mobility and number of mobile charge carriers, there has been no accurate method developed to determine these two quantities independently. In this paper, we apply a mean-field method based upon low frequency a.c. impedance measurements of the limiting low frequency space charge polarization capacitance that develops as a result of the mobile carrier population diffusing to blocking electrodes. The space charge capacitance that develops is shown to be a simple function of the number of charge carriers and is found to be independent of the d.c. conductivity, but strongly dependent upon temperature. Measurements on two simple but well studied ion conducting glasses,  $\text{LiPO}_3$  and  $\text{NaPO}_3$ , suggest that the carrier population is thermally activated where only a small fraction of the cations are mobile in the glass. The activation energy for carrier creation in  $\text{LiPO}_3$  is larger (49 kJ/mol) than that for  $\text{NaPO}_3$  glass (44 kJ/mol) and is in agreement with models of activation energies in ion conducting glasses that associate the creation energy with the cation charge density.

## Keywords

Space Charge Polarization, Cations, Ion Conducting Glasses

## Disciplines

Materials Science and Engineering

## Comments

This article is from *Zeitschrift für Physikalische Chemie* 223 (2009): 1379, doi: 10.1524/zpch.2009.6085.  
Posted with permission.

# Space Charge Polarization Measurements as a Method to Determine the Temperature Dependence of the Number Density of Mobile Cations in Ion Conducting Glasses

By Steve W. Martin\*, Wenlong Yao, and Kyle Berg

Department of Materials Science, Iowa State University of Science & Technology, Ames IA 50011–2300

*Dedicated to Prof. Dr. Klaus Funke on the occasion of his 65<sup>th</sup> birthday*

(Received September 11, 2009; accepted October 6, 2009)

## *Space Charge Polarization / Cations / Ion Conducting Glasses*

A method is proposed using mean-field theories to help solve a long standing problem in the study of ionically solid electrolytes. While it has been long known that the ionic conductivity in solid electrolytes is comprised of two terms, the mobility and number of mobile charge carriers, there has been no accurate method developed to determine these two quantities independently. In this paper, we apply a mean-field method based upon low frequency a.c. impedance measurements of the limiting low frequency space charge polarization capacitance that develops as a result of the mobile carrier population diffusing to blocking electrodes. The space charge capacitance that develops is shown to be a simple function of the number of charge carriers and is found to be independent of the d.c. conductivity, but strongly dependent upon temperature. Measurements on two simple but well studied ion conducting glasses,  $\text{LiPO}_3$  and  $\text{NaPO}_3$ , suggest that the carrier population is thermally activated where only a small fraction of the cations are mobile in the glass. The activation energy for carrier creation in  $\text{LiPO}_3$  is larger (49 kJ/mol) than that for  $\text{NaPO}_3$  glass (44 kJ/mol) and is in agreement with models of activation energies in ion conducting glasses that associate the creation energy with the cation charge density.

## 1. Introduction

The long standing and difficult problem that still remains in the otherwise very successful study of fast ion conducting (FIC) glasses has been to develop a

---

\* Corresponding author. E-mail: swmartin@iastate.edu

method to separately determine the number and mobility of the mobile carriers in these highly conducting glasses[1,2,3,4,5,6,7,8,9]. It is well accepted[10,11] that the conductivity can be written as the product of the charge on the carrier and the number and mobility of the charge carriers as given Eq. (1):

$$\sigma_{d.c.}(T) = n(T)eZ_c\mu(T) = \frac{\sigma_o}{T} \exp\left(\frac{-\Delta E_{act}}{RT}\right) \quad (1)$$

where  $\sigma(T)$  is the temperature dependent d.c. conductivity and  $n(T)$  is the temperature dependent number of carriers whose temperature dependent mobility is  $\mu(T)$ . In this expression that has its roots in the original Nernst-Einstein equation[10], we recognize that it has been found by Moynihan[12] and others[13] that the leading  $1/T$  dependence is often not well fit to the temperature dependence of the data and for this reason it is often not included in Arrhenius plots of the conductivity. We include it here for theoretical rigor, but also recognize that it does not strongly affect the values of the activation energies we find.

It is further well accepted that both the number and mobility of the charge carriers are individually thermally activated with individual activation energies. These are given in Eqs. (2) and (3), where  $\Delta E_c$  and  $\Delta E_m$  are the carrier and mobility activation energies

$$n(T) = n_o \exp\left(\frac{-\Delta E_c}{RT}\right) \quad (2)$$

$$\mu(T) = \frac{\mu_o}{T} \exp\left(\frac{-\Delta E_m}{RT}\right) \quad (3)$$

Combining Eqs. (1), (2), and (3), gives the widely accepted full expression for the temperature dependent ionic conductivity in ion conducting glasses.

$$\sigma_{d.c.}(T) = \frac{Z_c e n_o \mu_o}{T} \exp\left(\frac{-(\Delta E_c + \Delta E_m)}{RT}\right) \quad (4)$$

Equation (4) then shows that the total activation energy  $\Delta E_{act}$  is the sum of the two individual activation energy terms:

$$\Delta E_{act} = \Delta E_c + \Delta E_m \quad (5)$$

While it has been recognized that these energy barriers exist in ion conducting glasses, there have been few methods developed so far that have been able to provide independent measurements of these two activation energy terms. Approaches such as the weak electrolyte model[14] assume from the outset that it is the cation-anion dissociation process, controlled by  $\Delta E_c$ , that is the dominant of the two energy terms and as such is the dominant process controlling the ionic conductivity. The mobility of the ions is thought to have either no or at most a weak temperature dependence.

Structural models of these activation energies such as that due to Anderson and Stuart[15] or more recently due to Elliott[7] attempt to provide calculations of these energy barriers. While some progress can be achieved using these mod-

els, the short and long range disorder of the glass structure makes definitive calculations of these energy barriers using these models very difficult. Martin and Angell[16], however, some time ago did make some progress in at least relating these energy barriers to the structure of glass. The creation energy barrier,  $\Delta E_c$ , is associated with cation dissociation events initiating ion conduction. The migration energy barrier,  $\Delta E_m$ , is associated with conduction events that take the now dissociated ion over energy barriers in the glass structure that are associated with the volume requirements of the ion as it moves between ion sites. The creation energy barrier will decrease with an increase in the radius of the cation, moving from small  $\text{Li}^+$  ions to much larger  $\text{Cs}^+$  ions, for example, and with an increase in the radius of the charge compensating anion, moving from  $\text{O}^-$  to  $\text{S}^-$ , for example. The migration energy term will decrease with a decrease in the radius of the cation, but with an increase in the radius of the anion.

The main reason for the difficulty in separating these two terms lies in the relatively low mobility of the mobile ions. For example, if it is assumed that all of the cations in the FIC glass are mobile, for a typical room temperature conductivity of  $10^{-3} (\Omega\text{cm})^{-1}$  and a number density of  $10^{22}$  cations /  $\text{cm}^3$ , Eq. (1) gives a mobility of  $\sim 2 \times 10^{-7} \text{ cm}^2/\text{V}\cdot\text{sec}$ , cf.  $\sim \mu_H \sim 10^3 \text{ cm}^2/\text{V}\cdot\text{sec}$  for electrons in Si. Such small values make traditional Hall effect measurements very difficult where Hall voltages of  $\sim 1$  nV are predicted. This compares to  $\sim 200$  nV Seebeck voltages expected for copper wire contacts on a glass with only a 0.001 K temperature difference between the contacts. Indeed, to this author's knowledge, only limited Hall effect measurements have been made, those due to Dianoux et al. on the FIC glass  $z\text{AgI} + (1-z)\text{AgPO}_3$ [17], on the FIC crystal  $\alpha\text{-AgI}$ [18] by Funke et al., and two on the FIC crystal  $\text{RbAg}_4\text{I}_5$ [19,20].

To overcome these difficulties, alternative methods have been proposed over the years to use simpler less error prone methods. For example, the different temperature dependence between the d.c. conductivity and a.c. conductivity at some characteristic frequency, often taken to be where the a.c. conductivity reaches a value of twice that of the d.c. conductivity, is used to assign the typically lower activation energy of the a.c. conductivity to that of the mobility activation energy and by difference using Eq. (5) to determine the carrier activation energy[21]. However, this method is empirical based and relies on various assumptions, like, for example, the a.c. conductivity activation energy being attributed to only the migration activation energy and such *a priori* assumptions are not well founded nor supported.

Other techniques such as NMR would be expected to hold promise but unfortunately the cations of interest,  $\text{Li}^+$  and  $\text{Na}^+$  are quadrupole nuclei and as such are not readily amenable to quantitative NMR techniques[22]. The  $\text{Ag}^+$  cation, on the other hand, while spin  $1/2$  has such a low frequency and sensitivity which makes it very difficult to obtain  $^{109}\text{Ag}$  NMR spectra in the first place and even more difficult to obtain quantitative spectra[23].

For these reasons, we have explored still other techniques and report here one technique based upon the space charge polarization (SCP) that develops in

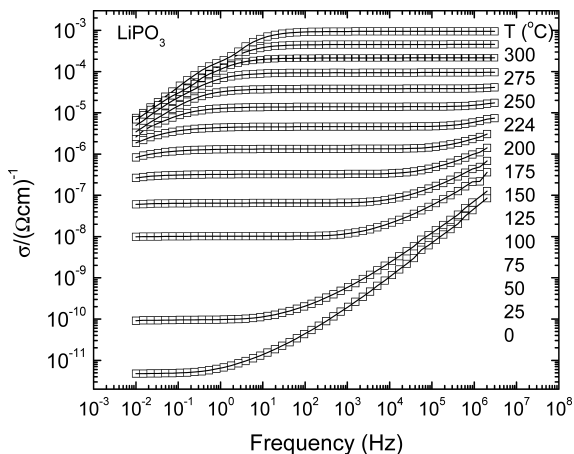


**Fig. 1.** a.c. conductivity data for a  $\text{LiPO}_3$  glass as a function of temperature. The data shows the three typical regions of frequency dependence of the a.c. conductivity. At low frequency where  $\tau_\sigma \ll 1/\omega$ , the conductivity is an increasing function of frequency due to the SCP processes. In the intermediate range of frequencies,  $\tau_\sigma \sim 1/\omega$ , the conductivity reaches the so-called d.c. plateau region. At the highest frequencies,  $\tau_\sigma \gg 1/\omega$ , the conductivity exhibits a power-law dependence. It is the low frequency SCP dominated region that is rarely if ever used and is often discarded or not even shown.

these electrolytes when measured with a low frequency ( $< 100$  Hz) a.c. voltage. The SCP is observed in almost all impedance spectroscopy measurements of FIC electrolytes, most commonly observed as a strongly decreasing a.c. conductivity in isothermal frequency scans, an example of which is shown in Fig. (1) for one of the glasses examined in this study. However, quite surprisingly, in most publications of FICs the SCP has been largely ignored at best or completely removed from the data at worse. Indeed, the only instance where it is often used to good purpose is in the determination of the d.c. conductivity of optimized FIC electrolytes where the high conductivity produces such strong SCP effects that the d.c. conductivity is completely masked by the SCP effect and in these cases, the SCP induced spike in the complex plane plots of the impedance is extrapolated to the real impedance axis to determine  $\sigma_{d.c.}(T)$ .

In this paper, we report a technique using mean-field theories where the SCP is purposely exploited to good effect to determine the charge carrier number density. Within the constraints and approximations of mean-field theory, it can be shown below that the SCP capacitance depends only upon the number of charges generating the SCP capacitance and the geometry of the sample and not on the conductivity. As a result, the temperature dependence of the SCP capacitance can be shown to arise only from the carrier or creation energy,  $\Delta E_c$ . Furthermore, the Arrhenius temperature dependence of the frequency below which the SCP begins to decrease is found to agree well with the Arrhenius temperature

dependence of the d.c. conductivity. Hence, in one experiment, the number, mobility, and d.c. conductivity of mobile ions in FIC electrolytes can be separated. This achieved by separately measuring the magnitude and temperature dependence of the limiting low frequency SCP (to determine the carrier number and carrier activation energy) and by measuring the onset frequency (or equivalently the mid-point frequency) of the SCP region.

In this our first report of this method, we have chosen one of the most widely and thoroughly studied of all ion conducting glasses, the alkali metaphosphates,  $\text{MPO}_3$ . The Li and Na metaphosphate glasses have been chosen because the ionic radii differences between  $\text{Li}^+$  and  $\text{Na}^+$  are expected to give systematic differences between the creation and migration energy barriers and these should show up in SCP measurements of them.

## 2. Mean-field theory of space charge polarization

The knowledge of and the theories for the SCP development in ionically conducting solids have been known for some time. As early as the 1950s, Proctor and Sutton[24] made accurate measurements of the SCP development in ion conducting alkali silicate and alkali-free non-insulating lead silicate glasses. Since then, Beaumont and Jacobs[25] and MacDonald[26,27] developed theories for the SCP under conditions of single alkali ion conductors in alkali silicate glasses and similar electrolytes. While Tomozawa and Shin[28] used the theory of Beaumont and Jacobs to determine the number of mobile protons in their relatively low proton concentration silicas, the technique appears to never have been applied to any FIC solid electrolyte. Indeed, to this author's knowledge, there have been no measurements of the SCP in FIC electrolytes for any purpose other than to use it as an aid in extracting the d.c. conductivity in the presence of the strong SCP behavior. There have been reports of SCP behavior also in ionic liquids (ILs) and work by Sangoro et al.[29], for example, shows that the behavior of these ionically conducting liquids is similar to the glasses being studied here, except that these ILs are essentially fully ionized and nearly all ionic species contribute to the conductivity. We will see below that the ionic glasses are only weakly ionized.

MacDonald's more recent theory[27], and his various improvements[26], have the flexibility of treating conductors that may have electrodes that are not completely blocking and the case where there may be more than one mobile carrier, such as either two cations (or anions) or the more common example of simultaneous anion and cation conduction. His theory collapses to the simpler Beaumont and Jacobs' theory in the limit of completely blocking electrodes and single carrier conductivities. In our present case where we are using Au sputtered electrodes at low voltages (50 mV) and single alkali conducting glasses, the two theories are identical.

Beaumont and Jacob[25] showed that in the case of SCP processes arising from the diffusion of single mobile cations in an ionic conductor whose base conductivity is  $\sigma$ , thickness is  $L$ , blocking factor  $\rho$  ( $= 0$  for completely blocking electrodes),  $\omega = 2\pi f$ , and whose limiting high frequency (electronic contributions only) dielectric constant is  $\epsilon_\infty$ , the real and imaginary parts of the dielectric constant could be represented as:

$$\epsilon_{sc}'(\omega) = \epsilon_\infty + \frac{2\epsilon_\infty(D^2K_1^3/\omega^2L)}{1+(2+\rho)^2(D^2K_1^2/\omega^2L^2)} \quad (6)$$

$$\epsilon_{sc}''(\omega) = \frac{\sigma_{dc}}{\omega\epsilon_0} - \frac{2\epsilon_\infty(D^3K_1^4/\omega^3L^2)(2+\rho)}{1+(2+\rho)^2(D^2K_1^2/\omega^2L^2)} \quad (7)$$

In both expressions,

$$K_1^2 \equiv \frac{n(T)e^2}{kT\epsilon_0\epsilon_\infty} \quad (8)$$

and

$$D(T) \equiv \frac{\sigma_{dc}(T)kT}{n(T)e^2} \quad (9)$$

Substituting  $K_1$ , Eq. (8), and the diffusion coefficient  $D$ , Eq. (9), into Eq. (6) gives:

$$\epsilon'(\omega) = \epsilon_\infty \left( 1 + \frac{2\sigma_{dc}^2(T) \sqrt{\frac{kT}{n(T)e^2(\epsilon_0\epsilon_\infty)^3}} \left( \frac{1}{\omega^2L} \right)}{1+(2+\rho)^2 \left( \frac{\sigma_{dc}^2(T)kT}{n(T)e^2\epsilon_0\epsilon_\infty} \right) \frac{1}{\omega^2L^2}} \right) \quad (10)$$

Now taking the low frequency limit,  $\omega \rightarrow 0$ , of this result to determine the SCP limiting value gives:

$$\epsilon_{sc} \equiv \lim_{\omega \rightarrow 0} \epsilon'(\omega) = \epsilon_\infty + \frac{2L\epsilon_\infty}{(2+\rho)^2} \sqrt{\frac{n(T)e^2}{kT\epsilon_0\epsilon_\infty}} \quad (11)$$

In comparing Eq. (10) to Eq. (11), it is seen that while Eq. (10) explicitly contains the d.c. conductivity,  $\sigma(T)$ , Eq. (11) does not. Rather, Eq. (11) contains only the number density of the mobile charge carriers,  $n(T)$ . It is in this way that it will be possible to test the hypothesis that the SCP can be used to determine the mobile carrier density in FIC glasses.

However, direct fits of Eq. (10) to the permittivity data of ion conducting glasses is quite poor due to the fact that the Beaumont and Jacobs model is a single relaxation time theory and further does not account for the internal conductivity polarization processes due to ion motion over a distribution of energy barriers. The most important feature of Eqs. (10) and (11), however, is not the frequency dependence of them (these can be corrected with appropriate attention), but rather the prediction of the low frequency limiting behavior, Eq. (11). The prediction is that if  $\epsilon_{sc}$  can be accurately determined from the experi-

mental data as a function of temperature, it can be used to calculate the temperature dependence of the number density of the charge carriers in the glass.

This is the strategy taken in the present work. Rather than try to include the higher frequency effects discussed above into the Beaumont and Jacob's theory, the alternate strategy is taken where the experimental permittivity data are first best-fit to a complete and accurate electrical circuit model of the electrical properties of the FIC glass that includes the limiting space charge polarization capacitance and the distribution of relaxation times behavior of the conductivity relaxation process with a limiting high frequency permittivity behavior. To fit the data in this manner, any number of least square impedance spectroscopy fitting routines could be used. Due to its robustness, ease of use, and accuracy, we chose to use the modeling software due to Macdonald, his LEVM package, see for example, ref. [30].

The modeling of the temperature and frequency dependence of the permittivity can be used to give accurate values the space charge induced capacitance,  $C_{sc}$ . From these values, the temperature dependence of the limiting low frequency space charge induced permittivity  $\epsilon_{sc}$ , can be determined. Using Eq. (11) with  $\epsilon_{sc}$  as an input value from the fitting of the dielectric data, the number density of mobile charge carriers were determined.

### 3. Experimental methods

#### 3.1 Preparation of the glasses

The glass compositions prepared in this study were made by melting stoichiometric amounts of high purity  $\text{Na}_2\text{CO}_3$ ,  $\text{Li}_2\text{CO}_3$ , and  $(\text{NH}_4)_2\text{HPO}_4$ . The carbonates decompose to the oxides evolving  $\text{CO}_2$  and the  $(\text{NH}_4)_2\text{HPO}_4$  decomposes to the oxide  $\text{P}_2\text{O}_5$  evolving  $\text{NH}_3$  and  $\text{H}_2\text{O}$ . Stoichiometric ratios of  $\text{M}_2\text{O}$  to  $\text{P}_2\text{O}_5$  yield the appropriate composition of  $\text{MPO}_3$ .

Samples for the conductivity experiments were annealed at  $T_g = -50^\circ\text{C}$  for thirty to sixty minutes and then allowed to cool to room temperature at  $5^\circ\text{C}/\text{min}$ . The disks were carefully dry polished inside the glove box to 4000 or 6000 grit using SiC polishing papers. This polishing was required to obtain reproducible polarization data at low frequencies. The polished glass discs were then sputter coated with a layer of platinum and then a layer of gold on both sides to form blocking electrodes for the conductivity experiments.

#### 3.2 Space charge polarization measurements

The permittivity data were collected using impedance spectroscopy measurements that were specifically optimized for low temperature collection of the data. The magnitude and phase of the impedance were collected using a Novocontrol a.c. impedance spectrometer[31]. The measurements were made by applying a

sinusoidal voltage (50 mV) across the sample. Measurements were made from 0 °C to 300 °C over a frequency range of 0.002 Hz to 10 MHz. The temperature was controlled to within  $\pm 0.5^\circ\text{C}$  by placing the sample into a specially designed wide temperature range cryostat capable of reaching temperatures as low as 100 K to as high as 673 K. Temperature control was accomplished by passing  $\text{N}_2$  gas through a heat exchange tube. Temperature scans were made every  $\sim 10^\circ\text{C}$ . Individual frequency scans were not started until the standard deviation of the temperature was within  $0.07^\circ\text{C}$  for the last 30 points measured every 2 seconds. The total time for the frequency sweep of the impedance was greater than one hour for frequency scans that started at and below 0.001 Hz and for this reason the frequency scans were started at 0.002 Hz. Even still, the frequency scans took  $\sim 1/2$  hour and for this reason, special attention was paid to ensure good temperature stability at all temperatures. The impedance magnitude and phase data were converted to the real and imaginary parts of the impedance, the a.c. conductivity, and the permittivity using standard expressions.

#### 4. Results and discussion

Figure (1) shows the a.c. conductivity data for  $\text{LiPO}_3$  glass, a similar plot is seen for  $\text{NaPO}_3$  and three regions of the frequency behavior of the conductivity are clearly observed. At lowest frequencies and highest temperature, the strongly decreasing conductivity with frequency is associated with the effects of SCP. In this region of frequency, the mobile ions have sufficient time,  $\tau_\sigma \ll 1/\omega$ , to diffuse significant distances in the sample before the electrical field is reversed and in doing so, create the SCP region. The region of charge of sign opposite to that at the electrodes arising from the applied field therefore significantly decreases the net field inside the sample and therefore also reduces the resulting current which in turn causes the apparent impedance of the sample to increase. As the frequency is increased, so the cations have progressively less time to create an SCP region and so the impedance decreases. At higher frequencies,  $\tau_\sigma \sim 1/\omega$ , the conductivity reaches the so called “d.c. plateau” region and the conductivity exhibits little or no frequency dependence. At still higher frequencies,  $\tau_\sigma \gg 1/\omega$ , the conductivity exhibits the well studied power law behavior whose origin is still of considerable debate and will not be further discussed here, see for example ref. [32].

Figures (2) and (3) show the wide frequency range determination of the real part of the dielectric constant,  $\epsilon'(\omega)$  for the  $\text{LiPO}_3$  and  $\text{NaPO}_3$  glasses. Also seen on these plots are the best-fit lines through the data which were calculated using the LEVM modeling software.

The data of Figures (2) and (3) show the general trends expected for a low frequency SCP dominated process. The dielectric constant at highest frequency is ascribed to the limiting high frequency dielectric constant,  $\epsilon_\infty$ . The dielectric constant then increases with decreasing frequency in the intermediate frequency

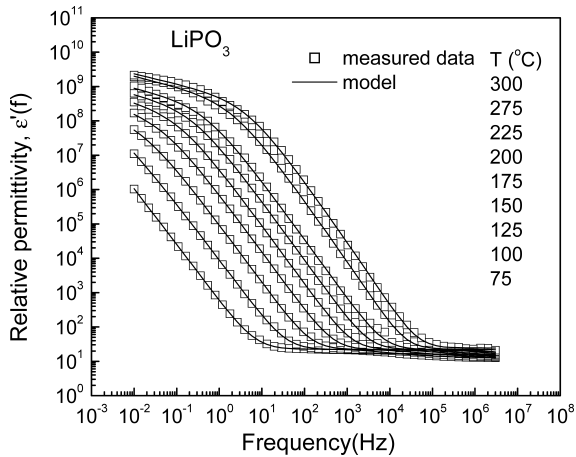


**Fig. 2.** Plot of the real part of the permittivity for the ion conducting  $\text{LiPO}_3$  glass as a function of both temperature and frequency. The lines are best-fits to the data using the LEVM equivalent circuit model as described in the text, parameters for the fits for each temperature are given in Table 1. The model includes a distribution of relaxation times for the bulk conductivity relaxation at higher frequencies and a temperature dependent  $C_{SC}$ . From the best-fit values of  $C_{SC}$ ,  $\epsilon_{SC} = C_{SC}\epsilon_0 A/L$  values were calculated.

range due to internal cation relaxation processes; this behavior is seen most clearly in the lowest temperature data. This conductivity relaxation process has been ascribed to polarization charges near high energy barriers in the glass. Glasses are well known to exhibit a distribution of activation energies[33] and at these intermediate frequencies, mobile charges can create internal polarizations by accumulating near the high energy barrier sites or even the blocked conduction pathway sites[34]. At still lower frequencies, the dielectric constant exhibits a very strongly increasing behavior that is shifted to lower frequencies the lower the temperature. At the lowest frequencies, the dielectric constant reaches a nearly constant plateau region where it is a much more slowly changing function of frequency. The magnitude of the dielectric constant in the plateau region appears to be temperature dependent, the lower the temperature the lower the limiting low frequency dielectric constant. Such behavior is fully consistent with that predicted by the SCP Eqs. (10) and (11).

The fitting of the real part of the dielectric permittivity using the LEVM yielded values for the  $C_{SC}$  and these values of  $C_{SC}$  were converted to values of  $\epsilon_{SC}$  and from these values for each glass at each temperature, the values of  $n(T)$  were calculated using Eq. (11). Figure (4) and (5) show the comparative Arrhenius plots of  $n(T)$  and  $\sigma_{d.c.}(T)$  for each glass. The differences in the temperature dependences of these two quantities are quite evident. From best-fits of the straight lines through the data points, values for the total activation energy, the creation energy, and (by difference) the migration energy barriers for these two glasses were determined.

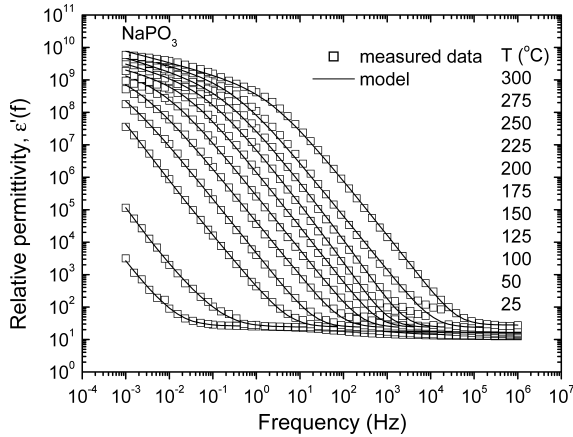


**Fig. 3.** Plot of the real part of the permittivity for the ion conducting  $\text{NaPO}_3$  glass as a function of both temperature and frequency. The lines are best-fits to the data using the LEVM equivalent circuit model as described in the text, parameters for the fits for each temperature are given in Table 1. The model includes a distribution of relaxation times for the bulk conductivity relaxation at higher frequencies and a temperature dependent  $C_{SC}$ . From the best-fit values of  $C_{SC}$ ,  $\epsilon_{SC} = C_{SC}\epsilon_0 A/L$  values were calculated.

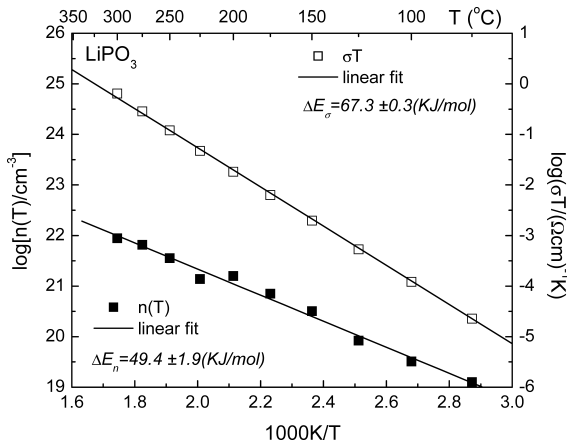


**Fig. 4.** Comparative Arrhenius plots of the d.c. conductivity,  $\sigma T$ , and the charge carrier number density,  $n(T)$ , for the ion conducting glass  $\text{LiPO}_3$ . The total conductivity activation energy is found to be 67.3 kJ/mol and the carrier creation activation energy is found to be 49.4 kJ/mol. The activation energy for the charge carrier number density give rises to a significantly smaller fraction of mobile carriers at any one temperature than the total, increasing from  $\sim 10^{-7}$  at  $\sim 100^\circ\text{C}$  to  $\sim 10^{-4}$  at  $350^\circ\text{C}$ . By difference, the carrier migration energy is 17.9 kJ/mol. Such behavior is consistent with the weak electrolyte approach where only a small fraction of the cations are mobile at any one temperature.

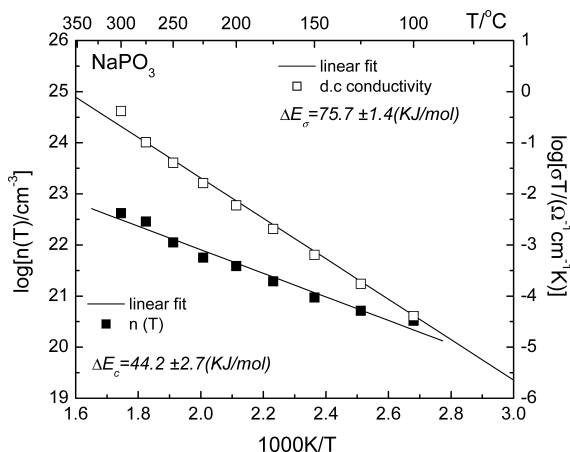


**Fig. 5.** Comparative Arrhenius plots of the d.c. conductivity,  $\sigma T$ , and the charge carrier number density,  $n(T)$ , for the ion conducting glass  $\text{NaPO}_3$ . The total conductivity activation energy is found to be 75.7 kJ/mol and the carrier creation activation energy is found to be 44.2 kJ/mol. By difference, the carrier migration energy is 31.5 kJ/mol. For the larger  $\text{Na}^+$  ion, the creation energy is smaller, but the migration energy is significantly larger and gives rise to an overall larger total conductivity activation energy. For the larger cations  $\text{Rb}^+$  and  $\text{Cs}^+$  the migration energy becomes so large as to make these cations immobile in the glassy state.

As expected from all of the models of the activation energies for conduction in glasses, the creation energy barrier is larger for the  $\text{LiPO}_3$  glass while it is smaller for the  $\text{NaPO}_3$  due to the smaller radii of the  $\text{Li}^+$  ion compared to that of the  $\text{Na}^+$  ion. In a similar way, the calculated migration energy barrier (by difference) is smaller for the  $\text{LiPO}_3$  glass than for the  $\text{NaPO}_3$ . From Figs. (4) and (5) it can be readily appreciated that the fraction of mobile ions in these glasses is relatively small, only approaching only  $\sim 100$  ppm at  $25^\circ\text{C}$  for  $\text{LiPO}_3$  and  $\sim 1000$  ppm at  $25^\circ\text{C}$  for  $\text{NaPO}_3$ . That these values are as low as they are is consistent with their relatively low overall conductivity and the relative strength of the alkali – oxide ionic bond strength. Similar measurements are in progress and will be reported soon on alkali ion conducting sulfide glasses where the alkali – sulfide bond strength is significantly weaker leading to significantly larger numbers of mobile cations and hence higher ionic conductivities.

The goal of this study was to use the low frequency permittivity data to good use rather than to discard it as it is typically considered a parasitic effect. The approach here was to determine if the magnitude of the limiting low frequency dielectric constant is consistent with that predicted from theories describing SCP processes arising from fast ion conduction of mobile cations to blocking electrodes.

As shown above, the low frequency behavior of the dielectric constants are fully consistent with the SCP theories. We have not, however, for sake of brevity spent any significant effort here to fully explore all the behaviors of the full

frequency dependence of the dielectric constant. This will be done in future publications.

The finding here is that the mobile ions are only weakly on average dissociated from their anionic charge compensating site, here non-bridging oxygens on  $-\text{O}-\text{P}(=\text{O})(\text{O}^-)-\text{O}-$  chain structures. The  $\text{LiPO}_3$  glass is observed to have the larger of the two,  $\sim 49$  versus  $\sim 44$  kJ/mole, creation energies, while the  $\text{LiPO}_3$  glass has the smaller of the two total conductivity activation energies, 67 versus 75 kJ/mole, respectively. This behavior while suggesting similarities to the weak electrolyte model, is perhaps more general and quantitative than the predictions of the weak electrolyte model. These values are also consistent with the values calculated for similar ionically conducting oxide silicate glasses where the mobile cations are charge compensated also by non-bridging oxygens, using either the much older Anderson-Stuart[15] or the more recent Elliott[7] models of conductivity activation energies where in all such calculations the creation or carrier number activation energy is the larger fraction of the total activation energy. For example, in binary sodium silicate glasses where the alkali ions are coulombically bound to oxygen anions, the Anderson-Stuart model gives a creation activation energy that is  $\sim 85\%$  ( $\sim 60$  kJ/mol) of the total activation energy (70 kJ/mol). By difference, the A-S strain energy for a sodium silicate glass is  $\sim 10$  kJ/mole. In the present cases, for  $\text{LiPO}_3$  the creation energy is  $\sim 66\%$  of the conductivity activation energy while for  $\text{NaPO}_3$ , this fraction decreases to  $\sim 59\%$ .

From Figs. (4) and (5), using the value of 49.4 kJ/mol for the carrier density activation energy and the d.c. conductivity activation energy of 67.3 kJ/mol gives a migration or strain activation energy barrier of 17.9 kJ/mol for the  $\text{LiPO}_3$  glass. Similarly, using the value of 44.2 kJ/mol for the carrier density activation energy and the d.c. conductivity activation energy of 75.7 kJ/mol gives a migration or strain activation energy barrier of 31.5 kJ/mol for the  $\text{NaPO}_3$  glass. As expected, the strain energy is larger for the larger  $\text{Na}^+$  cation. Due to the surprising fact that  $\text{KPO}_3$  is not a strong glass former, we have yet to examine this glass, but will in the future to extend this correlation on roller quenched compositions. The heavier alkali,  $\text{Rb}^+$  and  $\text{Cs}^+$  are so large as to show very little polarization due to the high strain energy effectively mitigating a sufficiently high conductivity.

Careful inspection of Figs. (4) and (5), however, do show perhaps a symptomatic problem with the mean-field approach used here. If one takes Eq. (2) above literally, then from Fig. (4) and (5), it is seen that the pre-exponential factor from the fit of the  $n(T)$  data for both  $\text{LiPO}_3$  and  $\text{NaPO}_3$  exceed the nominal value of the total concentration  $n_0$  for each of these glasses. Hence, one finds that for temperatures below the  $T_g$  of both of these glasses that the  $n(T)$  extracted from the Fig. (4) and (5) exceed the nominal value  $n_0$  for each of these glasses. This of course is an error caused by the use of the mean-field equations described and used above.

While the exact values for  $n(T)$  are likely to be over estimates of the actual number densities of the mobile cations, it perhaps more accurate and even more useful to consider their temperature dependencies. Seeing that the creation energies extracted from the analyses are in order of that expected for the smaller  $\text{Li}^+$  ions and the larger  $\text{Na}^+$  ions and also fit well with previous estimates of creation and migration energies for the well studied silicate glasses, as discussed above, this suggests that the creation energies as reported here are at least approximately correct and as such provide some of the very first measurements of these so far intractable energies.

In this way, both of these calculations, (modeling by AS and experiment here by SCP) perhaps show that as expected neither limiting case, strong or weak, of the electrolyte is the correct view. The creation and strain energy barriers are both non-zero and are significant fractions of the total activation energy. It is significant to note that the measurements and calculations reported here are consistent with reasonable expectations of the affect that the alkali and oxide chemistries would be expected to have upon the conduction energetics. That is the larger  $\text{Na}^+$  cation experiences smaller Coulombic energy barriers than those for the  $\text{Li}^+$  cation due to its larger radius. It is significant, however, that the coulomb energy barrier remains the larger of the two activation energy barriers. It is expected that for a smaller cation conducting glass, such as the  $\text{Li}^+$  cation, the creation energy would be larger and presumably also a larger fraction of the total activation energy. Likewise, for larger cations such as  $\text{K}^+$  and  $\text{Rb}^+$  the opposite might be true where the larger cations would produce a smaller creation energy barrier, but a larger strain energy barrier. In the future, we will report on systematic studies to examine not only these cation size effects in FIC glasses, but to also more fully examine the role of the anion size as well. Preliminary results are encouraging and are consistent with the results and discussion presented here. Comparative measurements will also be made on well studied and characterized crystalline FIC solid electrolytes such as  $\alpha\text{-AgI}$ , where, for example, the only reported Hall effect measurements of the ion mobility have been made and will allow accurate comparisons to the SCP measurements.

## 5. Conclusions

A mean-field method for determining the effective number of mobile cations in FIC glasses, in particular, and in single ion conducting electrolytes in general, has been suggested by measuring the low frequency SCP capacitance developed as a result of the mobile cations (ions) diffusing to blocking electrodes. This method uses the low frequency polarization data to good purpose. Two archetypical ion conducting glasses  $\text{LiPO}_3$  and  $\text{NaPO}_3$  were examined due to the large and previously existing knowledge base of these glasses as well as the slight but systematic differences in the ionic radii of the  $\text{Li}^+$  and  $\text{Na}^+$  cations. The SCP measurements of the creation (carrier) activation energy to be

$\sim 49.4 \pm 1.9$  kJ/mol for LiPO<sub>3</sub> and  $44.2 \pm 2.7$  kJ/mol for NaPO<sub>3</sub>. The measured total conductivity activation energies were found to be in agreement with those previously reported in the literature and were  $67.3 \pm 0.3$  kJ/mol and  $75.7 \pm 1.4$  kJ/mol, respectively. By difference, these values give estimates of the migration energy barrier of  $17.9 \pm 2.1$  kJ/mol and  $31.5 \pm 3.1$  kJ/mol, for LiPO<sub>3</sub> and NaPO<sub>3</sub> glasses, respectively. These values are found to be very consistent with calculations of these energy barriers using available models of conduction energetics in glass. It is therefore concluded from these measurements on these ion conducting glasses that while the dissociation of cations from their charge compensating anions sites appears to be the larger of the two activation energies, it is not the only activation energy and the migration (strain) energy must also be considered.

### Acknowledgement

This work was supported in part by the National Science Foundation through grants DMR-9972466 and DMR- IMI on New Functionality of Glass at Lehigh University and Pennsylvania State University. The authors would like to acknowledge helpful discussions with Professors Minoru Tomozawa (RPI), Klaus Funke (Muenster), Himanshu Jain (Lehigh), Bernhard Roling (Marburg), and J. Ross MacDonald (UNC-Chapel Hill) during the course of these measurements and the applications of the theories used in the analyses. Help in preparing the glasses and measuring their impedance spectroscopy was assisted by David Laughman at the University of Muenster, for whose help we are grateful. Partial support of this work therefore is acknowledged through the German Science Foundation through their support of the SFB 458 "Ionic Motion in Materials with Disordered Structures – From Elementary Steps to Macroscopic Transport"

### References

1. S. W. Martin, D. M. Martin, J. Schrooten, B. M. Meyer, *Journal of Physics: Condensed Matter* **15** (2003) S1643.
2. A. Pradel, N. Kuwata, M. Ribes, *Journal of Physics: Condensed Matter* **15** (2003) S1561.
3. K. Funke, R. D. Banhatti, S. Bruckner, C. Cramer, D. Wilmer, *Solid State Ionics* **154–155** (2002) 65.
4. C. A. Angell, *Solid State Ionics* **105** (1998) 15.
5. J. Swenson, R. L. McGreevy, L. Borjesson, J. D. Wicks, *Solid State Ionics* **105** (1998) 55.
6. M. Tatsumisago, *Yoyuen oyobi Koon Kagaku* **41** (1998) 191.
7. S. R. Elliott, *J. Non-Cryst. Solids* **172–174** (1994) 1343.
8. A. Pradel, M. Ribes, *Journal of Non-Crystalline Solids* **172–174** (1994) 1315.
9. M. D. Ingram, *Trends Non-Cryst. Solids, Proc. Int. Workshop Non-Cryst. Solids*, 3rd (1992) 385.
10. H. L. Tuller, D. P. Button, D. R. Uhlmann, *J. Non-Cryst. Solids* **40** (1980) 93.
11. S. K. Jain, H. C. Gaur, *Trans. Soc. Adv. Electrochem. Sci. Technol.* **11** (1976) 315.
12. C. T. Moynihan, D. L. Gavin, R. Syed, *Journal de Physique, Colloque* (1982) 395.

13. H. Jain, *Journal of Non-Crystalline Solids* **66** (1984) 517.
14. J. L. Souquet, W. G. Perera, *Solid State Ionics* **40–41** (1990) 595.
15. O. L. Anderson, D. A. Stuart, *J. Am. Ceram. Soc.* **37** (1954) 574.
16. S. W. Martin, C. A. Angell, *Journal of Non-Crystalline Solids* **83** (1986) 185.
17. V. Clement, D. Ravaine, C. Deportes, R. Billat, *Solid State Ionics* **28–30** (1988) 1572.
18. K. Funke, R. Hackenberg, *Berichte der Bunsen-Gesellschaft* **76** (1972) 883.
19. C. H. J. Stuhmann, H. Kreiterling, K. Funke, *Physical Chemistry Chemical Physics* **3** (2001) 2557.
20. C. H. J. Stuhmann, H. Kreiterling, K. Funke, *Solid State Ionics* **154–155** (2002) 109.
21. D. P. Almond, G. K. Duncan, A. R. West, *Solid State Ionics* **8** (1983) 159.
22. B. Meyer, F. Borsa, D. M. Martin, S. W. Martin, *Physical Review B: Condensed Matter and Materials Physics* **72** (2005) 144301/1.
23. T. Akai, S. W. Martin, F. Borsa, *Physical Review B: Condensed Matter and Materials Physics* **63** (2001) 024303/1.
24. T. M. Procter, P. M. Sutton, *The Journal of Chemical Physics* **30** (1959) 212.
25. J. M. Beaumont, P. W. M. Jacobs, *Phys. Chem. Solids* **28** (1967) 657.
26. J. R. Macdonald, *The Journal of Chemical Physics* **58** (1973) 4982.
27. J.R. MacDonald, *The Journal of Chemical Physics* **29** (1958) 1346.
28. M. Tomozawa, D. W. Shin, *Journal of Non-Crystalline Solids* **241** (1998) 140.
29. J. R. Sangoro, A. Serghei, S. Naumov, P. Galvosas, J. Kaerger, C. Wespe, F. Bordusa, F. Kremer, *Phys. Rev. E: Stat. Nonlinear, Soft Matter Phys.* **77** (2008) 051202/1.
30. J. R. Macdonald, *Solid State Ionics* **176** (2005) 1961.
31. J. A. Schrooten, Ph. D., Thesis, Iowa State University, (2001)
32. K. L. Ngai, C. T. Moynihan, *MRS Bull.* **23** (1998) 51.
33. S. W. Martin, F. Borsa, I. Svare, *Proceedings - Electrochemical Society* **2000–32** (2001) 66.
34. M. D. Ingram, *Curr. Opin. Solid State Mater. Sci.* **2** (1997) 399.

